

2-Amino-7-nitro-fluorenes in Neat and Mixed Solvents—Optical Band Shapes and Solvatochromism

Venugopal Karunakaran, Tamara Senyushkina, Ginagunta Saroja,[†] Jürgen Liebscher, and Nikolaus P. Ernsting*

Department of Chemistry, Humboldt-Universität zu Berlin, Brook-Taylor-Strasse 2, D-12489 Berlin, Germany

Received: May 18, 2007; In Final Form: August 7, 2007

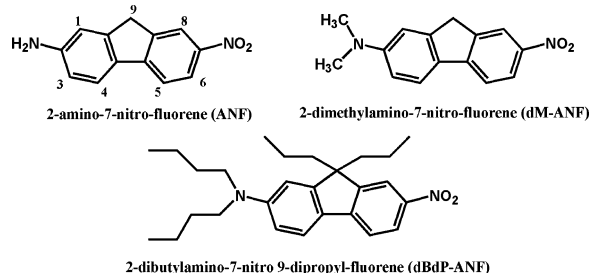
Femtosecond transient absorption spectroscopy of amino-nitro-fluorenes in the UV–visible range shows that the dynamic Stokes shift of the emission band is sensitive to infrared-active modes of the solvent. Bandshapes for stationary absorption and emission are needed to quantify the observed spectral evolution. They are reported for 2-amino-7-nitro-fluorene (ANF), 2-dimethylamino-7-nitro-fluorene (dM-ANF), and 2-di(n-butyl)amino-7-nitro-9-di(n-propyl)-fluorene (dBdP-ANF) in a variety of solvents. Bands broaden systematically with increasing solvent polarity. This effect is taken into account in an improved location of band positions. The resulting solvatochromic plots differ significantly from those that use peak positions of absorption spectra and fluorescence quantum distributions. Absorption spectra were also measured in aqueous solvent mixtures, and shifts are described by binding curves for hydrogen bonding and stepwise solvent exchange.

1. Introduction

The optical properties of 2-amino-7-nitro-fluorene (ANF, Scheme 1) were already studied by Lippert in his original work on polar solvation.¹ Excitation around 400 nm in the S_1 ($\pi\pi^*$) $\leftarrow S_0$ absorption band causes intramolecular charge transfer from the amino donor to the nitro acceptor group.² By modulating the absorption and emission bands in 1,4-dioxane with an electric field, Czekalla et al.³ determined dipole moments $\mu_0 = 6.4$ D in the electronic ground state and $\mu_1 = 20.3$ D in the excited state, which are essentially parallel. The molecule has C_s symmetry (see X-ray structure in the Supporting Information) in agreement with density-functional calculations.⁴ 2-(dimethylamino)-7-nitro-fluorene (dM-ANF, Scheme 1) was introduced by Catalan et al.⁵ who concentrated on UV–vis absorption spectra in more than 100 solvents and the gas phase. Methyl substitution of the amino hydrogen atoms removes sites of specific solvation. The peak position of the first dM-ANF absorption band may therefore be used as a parameter representing the dipolarity/polarizability of the medium.⁵

Specific⁶ and inhomogeneous^{7,8} solvation of ANF was characterized further by picosecond time-resolved fluorescence spectroscopy. In 2-propanol/benzene mixtures,⁶ the rates of Stokes shift and quenching by hydrogen-bonding interactions vary linearly with the mole fraction of 2-propanol. The Stokes shift is due to preferential solvation of the excited state by polar solvent molecules, increasing the microscopic dielectric constant above the macroscopic value. In ionic liquids, the Stokes shift depends on excitation wavelength.⁷ This observation implies a distribution of ground-state molecules differing in their interaction energies with the ionic liquid, and that solvation occurs on time scales longer than the S_1 lifetime in these media. It is consistent with molecular dynamics simulations, which gave an approximate time scale for reorganization of the solvent around the solute probe.⁸

SCHEME 1: Molecular Structures of Amino Nitro Fluorene Derivatives of This Study



The full potential of amino-nitro-fluorenes as solvation probes becomes apparent when the fluorescence band is observed with femtosecond time resolution. Emission from ANF in acetonitrile, for example, shifts to the red with a spectral oscillation or frequency modulation, which is quantitatively connected to the near-IR spectrum of the pure solvent.⁹ The oscillation reflects coherent solvent motion, which is launched by the sudden change of the solute dipole moment upon excitation. We did not observe this effect with the polarity probe Coumarin 153 (C153), which has many low-frequency modes.¹⁰ In order to see solvent oscillations, the chromophore should be rigid so that intramolecular wavepackets are avoided by excitation near the electronic origin.¹¹ Fluorene derivatives evidently are rigid and therefore will be used as probes for coherent solvent dynamics.

The most-practicable method to monitor a fluorescence band with femtosecond time resolution is transient absorption of a supercontinuum probe pulse.^{12,13} But transient absorption spectra are complex and must be decomposed into constituent bands. For example, consider dM-ANF in acetonitrile for which preliminary results are summarized in Figure 1. The upper panel shows spectra from 0 to 246 fs in steps of 12 fs, and arrows indicate spectral evolution. Excited-state absorption overlays the entire range, culminating in a sharp band at $22\,000\text{ cm}^{-1}$, which moves to the blue. Bleached absorption is indicated by negative induced optical density around $24\,000\text{ cm}^{-1}$ at earliest time. In the fluorescence region, stimulated emission is observed as an

* Corresponding author. E-mail: nernst@chemie.hu-berlin.de.

[†] Present address: School of Natural Sciences, Bedson Building, University of Newcastle upon Tyne, Newcastle upon Tyne, NE1 7RU, U.K.

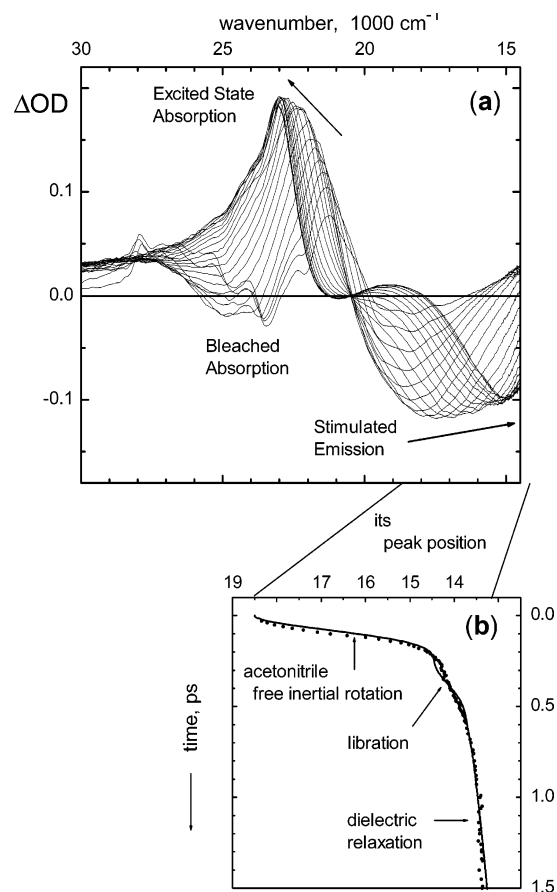


Figure 1. (a) Transient absorption ΔOD induced by optical excitation of 2-dimethylamino-7-nitrofluorene (dM-ANF) in acetonitrile. The negative-going band around $18\,000\text{ cm}^{-1}$ signifies stimulated emission; it may be converted into the corresponding fluorescence band. The evolution (arrows) is shown in 12-fs steps following 30 fs excitation at 400 nm. (b) Peak position of the band for stimulated emission as function of time after excitation (circles). A relaxation curve (line) was calculated from the far-infrared spectrum of pure acetonitrile. An oscillatory shoulder at 300 fs indicates a librational wavepacket in the solvent.

inverted band around $18\,000\text{ cm}^{-1}$, which moves to the red. The band becomes stationary at late time ($>3\text{ ps}$, not shown), and in this case it can be calculated from the spontaneous fluorescence spectrum. Its extraction for any given delay time t requires the stationary spectra of absorption and stimulated emission in the solvent (the procedure is explained in the supporting online material). Only then can a measure $\tilde{\nu}_x^{\text{fls}}(t)$ of the instantaneous $S_1 \rightarrow S_0$ energy gap in solvent x be defined. Experimental points in the lower panel, for example, identify $\tilde{\nu}_{\text{acn}}^{\text{fls}}(t)$ with the peak wavenumber of the stimulated-emission band. The solid line shows a relaxation curve, which was calculated from the FIR spectrum of pure acetonitrile using simple continuum theory.^{9,14} By comparison, a weak oscillatory shoulder at 300 fs can be assigned to coherent librational motion of surrounding acetonitrile molecules, reflecting the far-infrared absorption band in the neat liquid at 100 cm^{-1} , which broadly covers that region.

It follows that not only band positions but also bandshapes are needed if amino-nitro-fluorenes are to be used as dynamic solvation probes. The aim of this paper is to provide these bandshapes and to discuss them in view of extensive work by Catalan et al.⁵ Bands broaden systematically with increasing solvent polarity. This effect is taken into account in an improved location of solvatochromic band positions as devised by Fee

and Maroncelli.¹⁵ Aqueous mixtures are studied for later application to oligonucleotides in which a nucleobase has been exchanged for an ANF chromophore. Solvatochromic shifts that are induced by changing the composition are explained by correlation with amino ^1H NMR chemical shifts, and they are described by binding curves for hydrogen bonding and stepwise solvent exchange.¹⁶

2. Experimental Methods

The compounds were synthesized and purified as in ref 17. Water-soluble impurities were removed by washing a solution in chloroform repeatedly with water. All solvents were of UV grade (Merck UVASOL), and water had been deionized by exchange. For ANF in pure acetonitrile, the solvent had been dried and the solution was prepared under dry inert gas. Solvent mixtures were prepared by weight from the pure solvents and an aliquot from a stock solution of the dye ($1.5 \times 10^{-3}\text{ mol/L}$) in acetonitrile or dimethyl sulfoxide, respectively. In aqueous solutions the dye may precipitate, in which case the solid was removed by centrifugation. Solvent mole fractions x' were transformed to volume fractions x with the help of partial molar volumes.¹⁸ The temperature during optical measurements was $21 \pm 1\text{ }^\circ\text{C}$.

Absorption spectra, $\epsilon(\lambda)$, were recorded with a UV-vis scanning spectrophotometer (Shimadzu 3102PC). In case of low solubility, the optical path length was 10 cm; otherwise, 1 cm cells were used. Before each measurement, both the sample and reference cell were filled with the pure solvent or solvent mixture and a baseline was obtained. Fluorescence spectra were recorded upon excitation at the peak of the absorption band (absorbance ≤ 0.05). The collected photon flux, Φ , was dispersed in a double monochromator and registered by photon counting (Spex Fluorolog 212). Photometric calibration was performed with a secondary standard lamp (Optronic) in combination with the fluorescence from a series of dyes.¹⁹ In this way, the fluorescence quantum distribution $\partial\Phi/\partial\lambda \equiv F(\lambda)$ was obtained in each case. Wavelength axes were calibrated with a Hg lamp and He-Ne laser to $\pm 0.05\text{ nm}$ for absorption and $\pm 0.2\text{ nm}$ for emission. After moving to wavenumbers, $\tilde{\nu}$, spectra are presented as $\epsilon(\tilde{\nu})$ or $\partial\Phi/\partial\tilde{\nu} \equiv F(\tilde{\nu})$.

^1H NMR chemical shifts of ANF were measured in $\text{CD}_3\text{CN}/\text{H}_2\text{O}$ and $(\text{CD}_3)_2\text{SO}/\text{H}_2\text{O}$ mixtures (Bruker AM300). Solutions were prepared by volume with microsyringes for these experiments. Spectra were recorded for water volume fraction $x_{\text{H}_2\text{O}} \leq 0.3$ only because of low solubility at higher water content. Hexamethyldisiloxane (0.5%) in CCl_4 was used as an external standard in a sealed thin capillary inside the NMR tube. Before measuring with H_2O , the shift upon addition of D_2O was monitored. Because of fast H/D exchange of amino protons, their signal was lost at $x_{\text{D}_2\text{O}} > 0.1$.

3. Results and Discussion

3.1. Bandshapes and Solvatochromism in Pure Solvents.

Figure 2 shows the optical spectra of ANF, dM-ANF, and dBdP-ANF in acetonitrile. Each panel gives the respective stationary absorption spectrum (solid black line), the stimulated emission spectrum $\sigma_{\text{SE}} \propto F(\tilde{\nu})/\tilde{\nu}^2$ obtained from fluorescence (solid black line), and the calculated time-zero stimulated emission spectrum¹⁵ (thick gray line, see below). For example, consider dM-ANF in panel b. The stimulated emission band should have its peak at $19\,580\text{ cm}^{-1}$ at time-zero and at $13\,440\text{ cm}^{-1}$ when stationary; hence, the Stokes shift is expected to be 6140 cm^{-1} . The observed Stokes shift can be read off of Figure 1b;

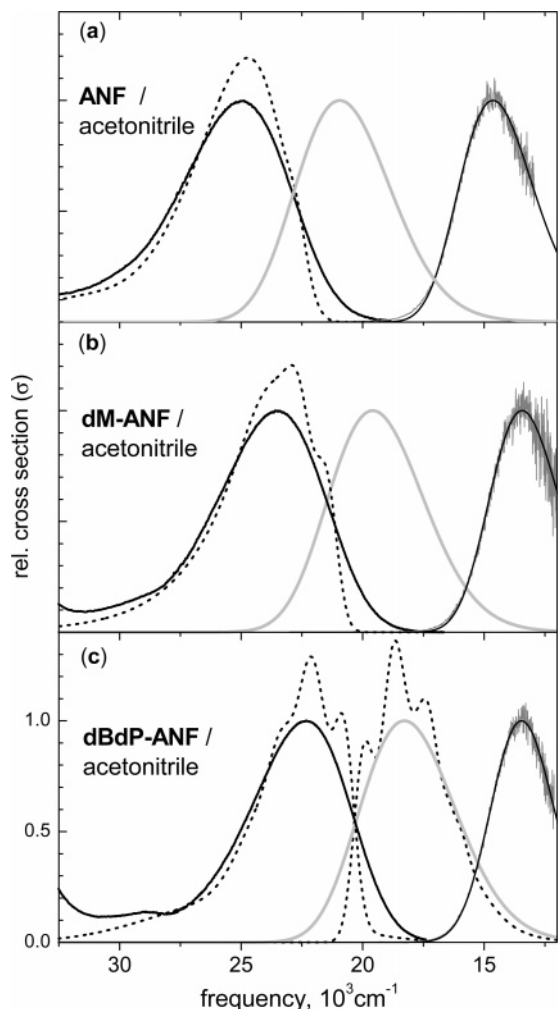


Figure 2. Optical spectra in acetonitrile: solid black lines, stationary absorption and stimulated emission (from fluorescence); thick gray, calculated time-zero stimulated emission; dashed lines, in 2-methylbutane, shifted such that Gaussian broadening gives the corresponding spectrum in acetonitrile.

it covers only 83% of the predicted value. An initial portion of the predicted Stokes is not observed, as will be discussed elsewhere.

Vibrational structure is not observed in polar solvents because of broadening that accompanies polar solvation. This effect can be seen for dBdP-ANF in Figure 2c where spectra in 2-methylbutane (2mb) are shown as dotted lines for comparison, but shifted so as to be optimally superimposed. Bands are structured and asymmetric in 2mb and unstructured, almost symmetric in acetonitrile (acn). Changing shape reflects a redistribution of electronic S_1-S_0 oscillator strength upon solvation. If no higher electronic state is coupled to S_1 , then the oscillator strength itself should be conserved. It follows that, regardless of application, optical spectra in the condensed phase should be described by the corresponding distribution of oscillator strength,²⁰ the normalized line shape function, which is for absorption

$$g(\tilde{\nu}) \propto \epsilon(\tilde{\nu})/\tilde{\nu} \quad (1)$$

and for emission

$$f(\tilde{\nu}) \propto F(\tilde{\nu})/\tilde{\nu}^3 \quad (2)$$

with $1 = \int f d\tilde{\nu} = \int g d\tilde{\nu}$. Line-shape functions were fitted by one or several lognormal functions²¹

$\text{lognorm}(\tilde{\nu}) =$

$$h \exp\left\{-\ln 2 \left(\frac{\ln[1 + 2\gamma(\tilde{\nu} - \tilde{\nu}_p)/\Delta]}{\gamma}\right)^2\right\} \quad (3)$$

with amplitude h , peak position $\tilde{\nu}_p$, width parameter Δ , and a dimensionless asymmetry parameter γ . The parameters for many solvents represent the essential data of this paper; they are available in the supporting online material. The parameters for solutions in 2mb are given in Table 1.

Band positions for absorption $S_1 \leftarrow S_0$ can be derived, in principle, from the corresponding line shape function directly by forming the average $\int \tilde{\nu} g(\tilde{\nu}) d\tilde{\nu}$. But absorption lineshapes $g(\tilde{\nu})$ may be uncertain at higher energy where transitions $S_n \leftarrow S_0$ are difficult to separate. Instead, we choose a method¹⁵ that refers to the underlying vibrational structure and gives the band position as the peak frequency of that structure. The absorption spectrum of dBdP-ANF in solvent $x = \text{acn}$ (Figure 2c) serves as example for the procedure. It is explained by the line shape measured in 2mb and shifted by $-\Delta\tilde{\nu}^{\text{abs}}$ (dashed line in the figure), then broadened by convolution with a Gaussian function $\propto \exp\{-1/2(\delta\tilde{\nu}/\tilde{\sigma}^{\text{abs}})^2\}$, which has fwhm $\tilde{\Gamma}^{\text{abs}} = \tilde{\sigma}^{\text{abs}}\sqrt{8\ln 2}$. By varying shift and broadening $\tilde{\sigma}^{\text{abs}}$, an optimal fit to the experimental data is sought over a frequency range that extends from the absorption peak by 900 cm^{-1} or $3\tilde{\sigma}^{\text{abs}}$ (whatever is larger) to the blue and red. Finally, one obtains

$$\tilde{\nu}_x^{\text{abs}} = \tilde{\nu}_{2\text{mb}}^{\text{abs}} - \Delta\tilde{\nu}^{\text{abs}} \quad (4)$$

where $\tilde{\nu}_{2\text{mb}}^{\text{abs}}$ is the peak frequency of the line shape for the compound in 2mb. For example, dBdP-ANF/acn is expected to have vibrational structure with maximum at $\tilde{\nu}_{\text{acn}}^{\text{abs}} = 22\,020 \text{ cm}^{-1}$ under the absorption line shape, while the peak of the broad absorption spectrum itself is located significantly higher at $22\,340 \text{ cm}^{-1}$.

The emission at time zero, immediately after excitation but before solvent relaxation, is estimated along similar lines.¹⁵ As before, one determines the shift and broadening that the absorption line shape experiences when the chromophore is transferred from 2mb to solvent x . Subsequently, these parameters are used to shift and broaden the emission line shape $f_{2\text{mb}}$. As a result, the emission line shape in solvent x at time zero, f_x^0 , is obtained. Such calculations²² gave the time-zero stimulated emission spectra, which are shown as gray lines in Figure 2.

Band positions for emission $S_1 \rightarrow S_0$ can be determined from the emission line shape directly. For this purpose, the average emission frequency in solvent x is formed:

$$\langle \tilde{\nu}_x^{\text{fls}} \rangle = \int \tilde{\nu} f_x(\tilde{\nu}) d\tilde{\nu} \quad (5)$$

From an analysis of dBdP-ANF emission lineshapes in aliphatic solvents, one finds that the peak emission frequency is located 693 cm^{-1} above the average. This relation should not be affected by Gaussian broadening; hence

$$\tilde{\nu}_x^{\text{fls}} = \langle \tilde{\nu}_x^{\text{fls}} \rangle + 693 \text{ cm}^{-1} \quad (6)$$

The derived properties $\tilde{\nu}_x^{\text{abs}}$, $\tilde{\Gamma}^{\text{abs}}$ and $\tilde{\nu}_x^{\text{fls}}$ are summarized in Table 2.

The peak extinction coefficient of ANF in acn was measured to be $\epsilon_{\text{max}} = 18\,373 \pm 100 \text{ L mol}^{-1} \text{ cm}^{-1}$. From our description for the $S_1 \leftarrow S_0$ absorption line shape (whose relative integral has an estimated error of $\pm 7\%$ because of overlap with higher bands), one obtains an electronic oscillator strength of $0.49 \pm$

TABLE 1: Lognormal Description of Optical Spectra (Oscillator Distributions) for the Dyes in 2-Methylbutane

dyes	absorption $g(\tilde{\nu})$				stat. fluorescence $f(\tilde{\nu})$			
	$\tilde{\nu}_p/\text{cm}^{-1}, \Delta/\text{cm}^{-1}, \gamma, h$				$\tilde{\nu}_p/\text{cm}^{-1}, \Delta/\text{cm}^{-1}, \gamma, h$			
	$S_n \leftarrow S_0$		$S_1 \leftarrow S_0$					
ANF	38115, 3080, 0.3674, 0.1237	25380, 854, 0.0048, 0.1225		22212, 1001, -0.0024, 0.6355 20965, 1225, -0.1020, 0.9629 19621, 1235, 0.0000, 0.7261 18513, 969, -0.0000, 0.3412 17663, 1473, -0.6582, 0.1847				
	41668, 6435, 0.1362, 0.4203	27309, 4072, 0.4053, 1.0000						
		34850, 4263, 0.2502, 0.0410						
dM-ANF	36999, 3275, 0.0978, 0.2803	23910, 1016, 0.0024, 0.5906		24902, 1174, 0.0047, 0.3560 25986, 3252, 0.6165, 0.8322 26491, 2199, 0.0117, 0.0583				
	40035, 4694, 0.4557, 0.2762	24292, 1416, 0.0084, 0.8190						
		25611, 1095, 0.0000, 0.2149						
dBdP-ANF	35969, 3271, 0.1124, 0.2347	23021, 996, 0.0024, 0.7066		25996, 2759, 0.0023, 0.3668 28050, 5745, 0.0159, 0.0934				
	39007, 4579, 0.4709, 0.2165	24292, 1416, 0.0084, 0.8190						
		25611, 1095, 0.0000, 0.2149						

TABLE 2: S_1-S_0 Frequencies $\tilde{\nu}$ (cm^{-1}) and Absorption Broadening Γ^{abs} (fwhm of Gaussian, cm^{-1}) for the Three Compounds in Various Solvents^a

solvent		n_D^b	ϵ_0^b	ANF			dM-ANF			dBdP-ANF		
				$\tilde{\nu}^{\text{abs}}$	Γ^{abs}	$\tilde{\nu}^{\text{fls}}$	$\tilde{\nu}^{\text{abs}}$	Γ^{abs}	$\tilde{\nu}^{\text{fls}}$	$\tilde{\nu}^{\text{abs}}$	Γ^{abs}	$\tilde{\nu}^{\text{fls}}$
perfluoro-n-hexane	pfh •	1.252	1.57	nm	nm	nm	nm	nm	nm	25 100	dd	19 290
2-methyl-butane	2mb •	1.3509	1.83	27 300	dd	nm	25 300	dd	nm	24 380	dd	20 940
n-pentane	pen •	1.3547	1.84	27 280	dd	nm	25 240	dd	nm	24 360	dd	20 950
n-hexane	hex •	1.3723	1.88	27 180	dd	nm	25 120	dd	nm	24 260	dd	20 840
n-heptane	hep •	1.3851	1.92	27 100	dd	nm	25 080	dd	nm	24 180	dd	20 780
n-octane	oct •	1.3951	1.95	27 020	dd	nm	24 980	dd	nm	24 140	dd	20 700
cyclohexane	ch •	1.4235	2.02	26 860	dd	nm	24 840	dd	nm	23 980	dd	20 600
carbon-tetrachloride	ctc •	1.457	2.24	26 320	1370	19 950	24 350 ^c	1480 ^c	19 330	23 430	1180	18 820
chloroform	chl	1.442	4.89	25 240	2730	16 500	22 740	2570	15 080	21 730	2350	14 780
1,1,1-trichloro-trifluoro-ethane	tctf •	1.356	2.41	26 860	1670	nm	24 750	1600	19 180	23 770	1320	18 660
diethyl ether	dee •	1.3495	4.20	25 140	2070	17 680	24 030	1670	16 840	23 300	1600	16 450
dipropyl ether	dpe •	1.3780	3.39	25 150	2170	17 470	24 050	1550	16 670	23 320	1440	16 160
dibutyl ether	dbe •	1.3968	3.08	25 550	2140	19 140	24 250	1250	18 720	23 480	1130	18 630
tetrahydro-furane	thf •	1.4050	7.58	24 310	2190	17 300	23 170	2120	16 460	22 480	1950	16 530
tetrahydro-pyrene	thp •	1.4186	5.61	24 380	2170	16 940	23 340	1950	15 960	22 630	1790	15 860
1,4-dioxane	dio	1.4203	2.21	25 090	2120	18 200	23 620	1950	17 400	22 890	1810	17 300
methyl acetate	mac •	1.3589	6.68	24 800	2430	16 970	23 390	2280	15 910	22 660	2120	16 450
ethyl acetate	eac •	1.3698	6.02	24 800	2330	17 300	23 470	2170	16 360	22 740	2000	16 040
dimethyl-formamide	dmf •	1.428	36.71	23 200	2730	14 880	22 310	2710	14 010	21 550	2570	14 120
hexamethyl- phosphoramidate	hmpa •	1.457	29.30	nm		15 540	22 230	2430	14 820	21 530	2380	14 890
dimethyl sulfoxide	dmsO •	1.477	46.45	22 720	2850	14 530	21 920	2850	13 620	21 210	2660	13 680
acetonitrile	acn •	1.341	35.94	24 600	2870	14 770	22 860	2900	13 710	22 020	2680	13 920
propionitrile	prn •	1.363	28.26	24 520	2760	14 730	22 880	2730	14 290	22 020	2500	14 310
methanol	meOH	1.3265	32.66	24 740	3910	14 550	23 140	3340	nm	22 280	2940	13 670 ^d
ethanol	etOH	1.3594	24.55	24 460	3720	15 110	23 200	2920	14 580	22 440	2780	14 400 ^d
propanol	proH	1.3837	20.45	24 470	3840	15 580	23 210	2940	14 880	22 460	2800	14 710 ^d
butanol	buOH	1.3974	17.51	24 470	3790	15 660	23 250	2900	14 930	22 490	2780	14 930 ^d
benzene	bz	1.4979	2.27	25 490	1770	19 320	23 420	1580	18 000	22 750	1410	17 990
toluene	tol	1.4941	2.38	25 540	1650	19 490	23 530	1460	18 340	22 870	1320	18 250

^a A full circle indicates use for solvatochromic regression analysis. dd = peak frequency determined directly so that Γ^{abs} was not obtained; nm = not measured. ^b Refractive index n_D and static dielectric constant ϵ_0 values are taken from the tabulations in Riddick, J.A.; Bunger, W.B.; Sakano, T.K. *Organic Solvents*; Wiley: New York, 1986. ^c Excess absorption on blue side. ^d Positive asymmetry.

0.035 and transition dipole moment of 6.33 ± 0.22 D. Using the fluorescence quantum distribution (see the Supporting Information), we find a radiative lifetime of 15.3 ns in acn.

The continuum theory of polar solvation is well established²³ (for recent use see ref 24). In its simplest version, the solute is represented by a point dipole with moment μ in a spherical cavity with radius a , and the surrounding liquid is treated as a continuum with dielectric constant ϵ and refractive index n . Both ANF and dM-ANF have been studied extensively in this context with pure solvents.¹⁻⁵ Here we add fluorescence spectra, and the previous work is complemented by two points that come into play because bandshapes are used in the analysis: (i) a link between band broadening and solvatochromic shift²⁵ and (ii) a systematic improvement of solvatochromic slopes that have been reported.⁵

The spectral positions of the absorption and fluorescence bands are²⁶

$$\tilde{\nu}_{\text{solvent}}^{\text{abs}} = \tilde{\nu}_{\text{gas}}^{\text{abs}} + \left[A + B + \frac{\mu_0^2 - \mu_1^2}{hca^3} \right] f(n) + \left[\frac{2\mu_0(\mu_0 - \mu_1)}{hca^3} \right] F(\epsilon, n) \quad (7)$$

$$\tilde{\nu}_{\text{solvent}}^{\text{fls}} = \tilde{\nu}_{\text{gas}}^{\text{fls}} + \left[A + B + \frac{\mu_0^2 - \mu_1^2}{hca^3} \right] f(n) + \left[\frac{2\mu_1(\mu_0 - \mu_1)}{hca^3} \right] F(\epsilon, n) \quad (8)$$

The first bracket together with $f(n) = \{n^2 - 1\}/\{2n^2 + 1\}$ describes the dispersion energy (A, B) and the energy needed

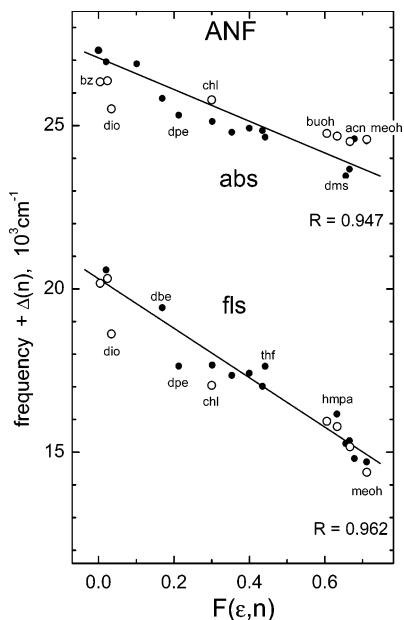


Figure 3. Frequency of ANF steady-state absorption and emission bands (peak frequency of oscillator distribution kernel, eqs 4 and 6) in a range of solvents, plotted vs the reaction field factor $F(\epsilon, n)$, eq 9. The effect of changing dispersion has been removed (see the text).

to induce solvent dipoles. It can be found separately from the $S_1 \leftarrow S_0$ absorption band in aliphatic solvents (slopes $s = -17\,296, -17\,358, -15\,529 \text{ cm}^{-1}$ for ANF, dM-ANF, and dBdP-ANF, respectively, with correlation coefficients >0.993). The second bracket describes the interaction between permanent solute dipoles and solvent dipoles. The reaction field factor or polarity function, $F(\epsilon, n)$, has various forms depending on how the solute polarizability, α , is treated. Here we take the form recommended²⁷ when its contribution is minor, that is, when the polarizability can be approximated as $\alpha \approx a^3/2$:

$$F(\epsilon, n) = \frac{\epsilon - 1}{\epsilon + 2} - \frac{n^2 - 1}{n^2 + 2} \quad (9)$$

The dependence of the spectra on $F(\epsilon, n)$ is shown in Figures 3 (ANF) and 4 (dBdP-ANF) and in the Supporting Information (dM-ANF). To take out the effect of solvent polarizability, the frequencies of Table 2 have been shifted to $\tilde{\nu} + \Delta(n) \equiv \tilde{\nu} + s(0.1774 - f(n))$ as if the refractive index were always that of 2mb. The ground- and excited-state dipoles are assumed parallel, and a term $\sim F^2$ for the solvent Stark effect has been omitted in eqs 7 and 8. Full circles represent all regular solvents, that is, those that cannot donate H bonds and are not strongly multipolar at first order (cf. Table 2). These points were used to calculate the linear regression lines, which are summarized in Table 3. Note that because of the definition of $F(\epsilon, n)$, the corresponding slopes contain the gas-phase dipole moments μ_0, μ_1 .

It is interesting to compare broadening $\tilde{\sigma}^{\text{abs}}$ to absorption shift $\Delta\tilde{\nu}^{\text{abs}}$ when the solute is transferred from 2-methylbutane to a polar solvent. Linear response of solvation implies

$$\frac{\tilde{\sigma}^{\text{abs} 2}}{k_B T/hc} = 2\Delta\tilde{\nu}^{\text{abs}} \quad (10)$$

where $k_B T$ is the thermal energy, h Planck's constant, and c is the light velocity. This relationship^{25a} has been demonstrated for C153,^{25b} in which case the full dynamic Stokes shift was used in place of $2\Delta\tilde{\nu}^{\text{abs}}$. Figure 5 shows the quantity on the

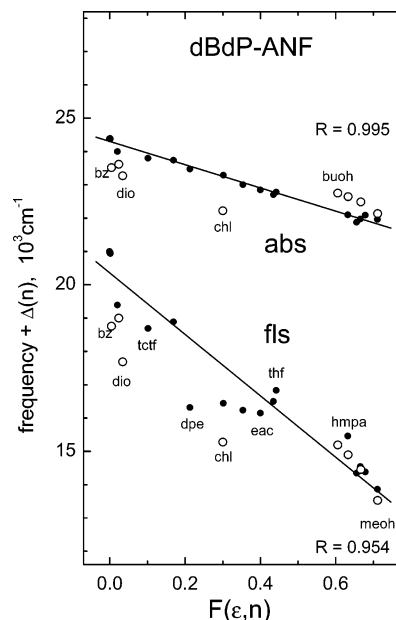


Figure 4. Frequency of dBdP-ANF steady-state absorption and emission bands in a range of solvents, as in Figure 3.

l.h.s. of eq 10 plotted against $\Delta\tilde{\nu}^{\text{abs}}$ for the three amino-nitrofluorenes in the “regular” solvents. The slope of a regression line through the origin is 2.18 ± 0.06 , thus confirming the validity of linear response in the electronic ground state, even though the correlation is not as strict as that with C153.

The systematic error that comes from using peak positions of absorption spectra and fluorescence quantum distributions can now be estimated. For this purpose, consider dBdP-ANF in Figure 4 and assume that the chromophore is transferred from 2mb to a solvent with polarity $F(\epsilon, n)$. The expected shifts $-\Delta\tilde{\nu}^{\text{abs}}$ and $-\Delta\tilde{\nu}^{\text{fls}}$ of the underlying vibronic lineshapes (Table 1) are calculated from the solvatochromic slopes (Table 3). The shifted lineshapes are then broadened by a Gaussian function with standard width $\tilde{\sigma}^{\text{abs}}$ or $\tilde{\sigma}^{\text{fls}}$, respectively, obtained by generalizing eq 10. After conversion to $\epsilon(\tilde{\nu})$ and $F(\tilde{\nu})$ (eqs 1 and 2), their peak positions are determined. Results are shown in Figure 6. The experimental absorption points in the corresponding Figure 4 adhere well ($R = 0.995$) to the linear regression line so that the deviation incurred when peaks of $\epsilon(\tilde{\nu})$ are used becomes significant. The experimental fluorescence points, however, scatter far from their regression line ($R = 0.954$), which is why a systematic error in using the peak of $F(\tilde{\nu})$ goes unnoticed. For example, in acetonitrile the peak of $F(\tilde{\nu})$ is expected to be 505 cm^{-1} higher in energy than the peak of the underlying emission line shape. These deviations must be considered when a well-behaved probe molecule with the same dipole-moment change is used to measure the local electric field strength.

3.2. Solvatochromism in Aqueous Solvent Mixtures. Figure 7 shows the absorption frequency of ANF (a) and dM-ANF (b) as function of the volume fraction, x , of the second component. Frequencies were determined by the underlying vibronic line shape function as described before. In this way, the effect of Gaussian broadening that accompanies increasing solvation by water is removed and even small spectral shifts can be tracked. In ideal mixtures, the dielectric properties depend linearly on the volume fraction, x , of the second component,²⁸ which is therefore adopted as a measure of composition. The mixtures were acn/water (circles), dms/water (squares), and acn/dms (triangles). The Kamlet–Taft acidity and basicity parameters^{29,30}

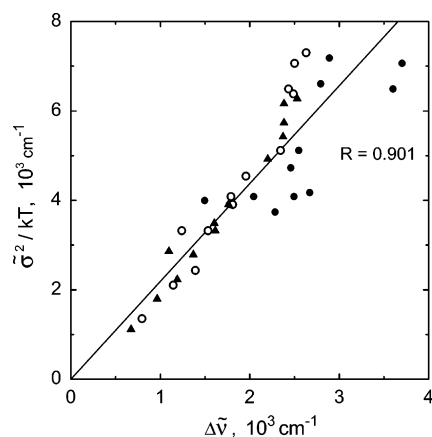


Figure 5. Test of the linear response relationship between the absorption shift $\Delta\tilde{\nu}^{\text{abs}}$ upon transfer from 2-methylbutane to a solvent, and the corresponding Gaussian broadening $\tilde{\sigma}^{\text{abs}}$ (see the text). ANF, full circles; dM-ANF, empty circles; dBdP-ANF, solid triangles.

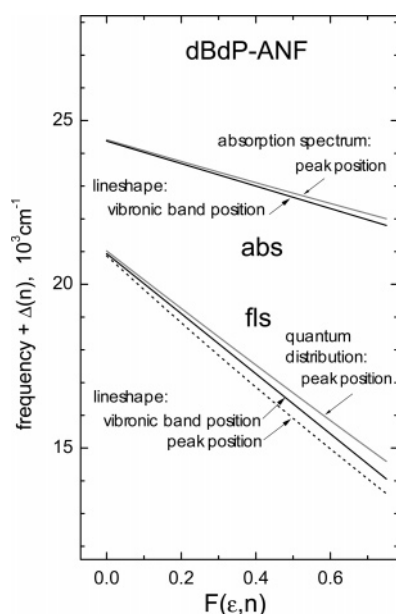


Figure 6. Solvatochromic plots using peaks of the absorption spectrum and fluorescence quantum distribution, as compared to using the peak of the underlying vibronic lineshapes.

α and β for the three pure solvents are 0 and 0.76 for dmsol, 0.19 and 0.31 for acn, and 1.17 and 0.18 for water. Dashed lines connect the values for the pure solvents, which were inferred from the corresponding absorption regression lines (Table 3). They represent the expected frequencies when only unspecific solvation is active (through solvent polarity and polarizability) obeying simple continuum theory. For the interpolation, it was assumed that ϵ and n change linearly with volume fraction x .

The behavior of dM-ANF in Figure 7b is discussed first, and for a start consider the acn/dmsol series (triangles). Dimethyl sulfoxide is slightly less polar ($F = 0.656$) than acetonitrile ($F = 0.711$), and for this reason the absorption band should shift to higher frequencies by about $+180 \text{ cm}^{-1}$ as x_{dmsol} is increased

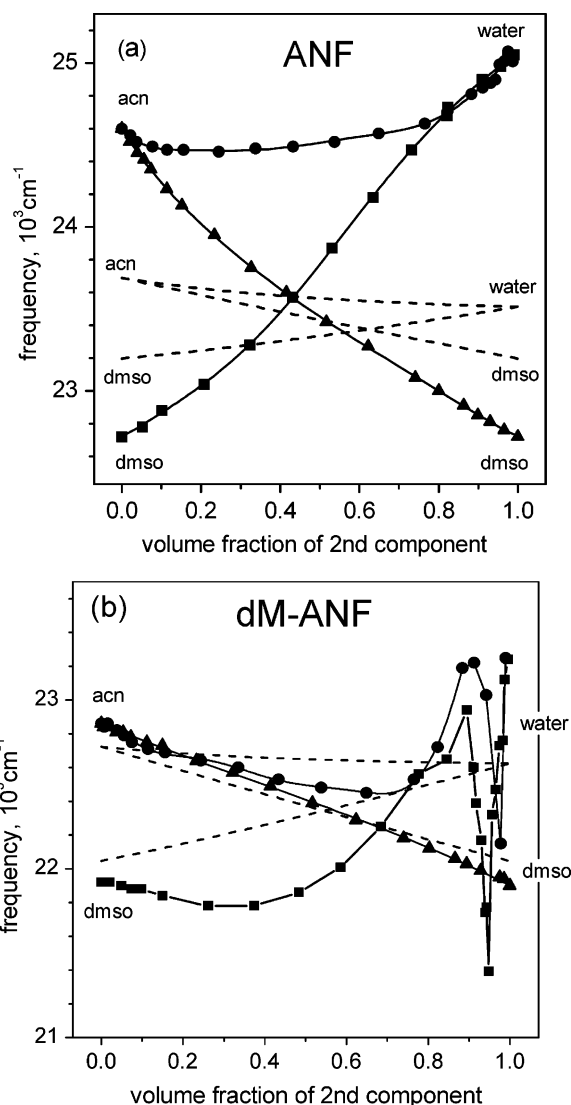


Figure 7. Absorption frequency in solvent mixtures, as function of volume fraction of the second component. (a) ANF, (b) dM-ANF. Dashed lines connect the points for the pure solvents, as expected from the solvatochromic regression analysis.

from 0 to 1. But at the same time, n increases from 1.341 to 1.477 and the net expected change becomes -680 cm^{-1} (appropriate dashed line in Figure 7b). The observed frequency falls on a straight line that starts above the expected line and then goes below.³¹ Hydrogen bonds cannot be formed between dM-ANF and dmsol; therefore, the deviations of $\pm 90 \text{ cm}^{-1}$ (between the dashed and solid lines) must be ascribed to solvation,³² which cannot be captured by a continuum model.

When water ($F = 0.757$) is added to a solution of dM-ANF in acn, simple theory predicts a small linear decrease of the absorption frequency (appropriate dashed line in Figure 7b), mainly because of polarity change in this case. The observed absorption frequency (circles and solid line) first moves gradually more to the red, reaches a minimum at $x_{\text{H}_2\text{O}} = 0.69$, then turns around and moves to the blue by more than 1300 cm^{-1} in

TABLE 3: Parameters (and Standard Errors) from the Solvatochromic Analysis in Figures 3 and 4 and the Supporting Information

dyes	$\tilde{\nu}^{\text{abs}} + \Delta(n) =$	$\tilde{\nu}^{\text{fls}} + \Delta(n) =$
ANF	$(27075 \pm 150) - (4852 \pm 400) F(\epsilon, n)$	$(20309 \pm 315) - (7569 \pm 648) F(\epsilon, n)$
dM-ANF	$(25187 \pm 42) - (3663 \pm 108) F(\epsilon, n)$	$(19718 \pm 316) - (8010 \pm 673) F(\epsilon, n)$
dBdP-ANF	$(24255 \pm 31) - (3433 \pm 79) F(\epsilon, n)$	$(20305 \pm 266) - (9168 \pm 678) F(\epsilon, n)$

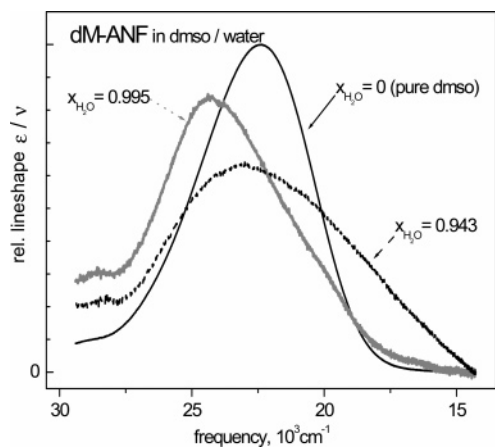


Figure 8. dM-ANF absorption lineshapes in dmsO/water. In a sharp compositional region around water volume fraction $x_{\text{H}_2\text{O}} \approx 0.94$ (dashed line) an absorption contribution appears to the red of band in pure dmsO, probably due to dimer formation.

the end. In dmsO/water (squares), similar behavior is seen on a larger vertical scale. One possibility to consider is preferential solvation, that is, the enrichment in the first few solvent shells of one component over the other. This effect can be described in basic thermodynamic terms by the stepwise solvent exchange,¹⁶ quasi-lattice quasi-chemical,³³ competition preferential,³⁴ and Kirkwood–Buff³⁵ theories. A more-molecular description was given by Suppan who considered that solvent dipoles interact differently with the dipolar solute.³⁶ Dielectric enrichment leads to an effective frequency that falls between those for the pure solvents. For example, in dmsO/water the initial slope should be zero if dmsO were completely retained.³⁷ The observed small decrease as $x_{\text{H}_2\text{O}}$ is raised to 0.4 is still consistent with this view, since the deviation ($<100 \text{ cm}^{-1}$) from a horizontal line is of the same size which earlier had to be ascribed to molecularity. We conclude that dM-ANF in dmsO/water it is completely surrounded by dmsO solvent shells up to $x_{\text{H}_2\text{O}} \approx 0.4$.

At the other end, a water-rich mixture has acn or dmsO as cosolvent. The strong blue-shift of dM-ANF absorption as $x_{\text{H}_2\text{O}} \rightarrow 1$ indicates weakened interaction in the excited state. The only mode available for this is a donated H bond to the dimethyl amino group. Upon $S_1 \leftarrow S_0$ excitation, electronic charge is drawn from the amino group and the interaction strength is thereby reduced. But as was mentioned before, the blue-shift becomes noticeable only from $x_{\text{H}_2\text{O}} \geq 0.4$ in dmsO/water and ≥ 0.7 in acn/water. It follows that specific solvation of the dimethylamino group by H_2O is not favored at lower water content.

An interesting feature is a narrow frequency dip as methyl-containing cosolvent is added to a solution of dM-ANF in (nearly) pure water. The compositional range was scanned in finer steps with dmsO/water (not shown), and the maximal effect is located around $x_{\text{H}_2\text{O}} \approx 0.94$ corresponding to a dmsO mole fraction of 0.016. Figure 8 shows the absorption band at this composition. Compared to solution in pure dmsO, the distribution of oscillator strength at $x_{\text{H}_2\text{O}} \approx 0.94$ has opposite asymmetry; that is, it slopes toward the red. Thus, a significant contribution to the oscillator strength comes from molecules that absorb at lower frequencies than in pure dmsO. At this stage, we can only speculate on the underlying cause³⁸ of the narrow frequency dip, which is also seen in acn/water but at slightly different composition. The possibilities are (i) specific solvation at the dimethyl amino and nitro caps of the molecule,³⁹ (ii) dimer formation,⁴⁰ and (iii) specific interaction between cosolvents.^{41,42}

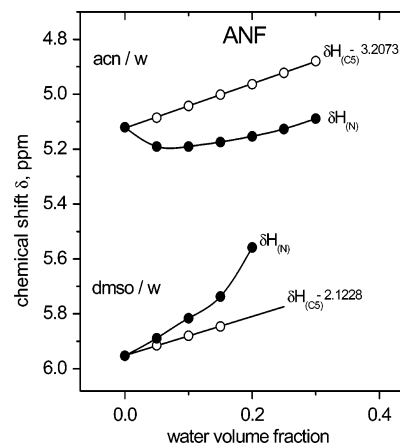


Figure 9. ^1H NMR chemical shift of amino protons $\delta H_{(\text{N})}$ in ANF as function of water volume fraction in $\text{CD}_3\text{CN}/\text{H}_2\text{O}$ and $(\text{CD}_3)\text{SO}/\text{H}_2\text{O}$. The behavior of a $\delta H_{(\text{CS})}$ resonance is shown shifted for comparison.

In either case, multiple equilibria between single dM-ANF molecules, water, and cosolvent must be involved, which are controlled by the thermodynamic properties of the bulk solvent mixture. The two aqueous solvent systems are interesting because the cosolvent disrupts the hydrogen-bonded water network.^{41,42} This is indicated by unusual thermodynamic properties. For example, dilute dimethyl sulfoxide in water contracts its partial molar volume to 96% of pure dmsO and has strongly negative excess entropy of mixing, in partial molar terms $\partial(TS^E)/\partial x'_{\text{dmsO}} = -12.68 \text{ kJ/mol}$.¹⁸ Taken together, it follows that differently absorbing species may depend highly nonlinearly on solvent composition, allowing for the observation of sharp absorption features when varying $x_{\text{H}_2\text{O}} \approx 1$.

The dependence of the ANF absorption band on solvent composition (Figure 7a) is discussed next. Now the band in pure dmsO is more red-shifted from its position in pure acn, when compared to dM-ANF, because dmsO accepts H bonds from the amino group and these become stronger upon $S_1 \leftarrow S_0$ excitation. Comparing the acn/dmsO curves for ANF and dM-ANF, the former bends significantly below an ideal straight line, whereas the latter stays just above. Unsurprisingly, this indicates preferential solvation of ANF by dmsO, including specific solvation of the amino group. One finds that half of the full shift of ANF in acn/dmsO is already achieved at $x_{\text{dmsO}} = 0.27$. The curve for ANF in dmsO/water looks qualitatively different from that for dM-ANF. Adding small amounts of water to ANF in dmsO should, in principle, affect two specific equilibria involving the amino group: exchange of H-bond-accepting dmsO ($\beta = 0.76$) for accepting H_2O molecules ($\beta = 0.18$) and donation of an H bond by H_2O ($\alpha = 1.17$). The latter process is unlikely to be dominant at low water content in view of the results with dM-ANF above. Therefore, exchange of stronger for weaker H-bond acceptors should characterize the initial part of the dmsO/water curve in Figure 7a. In contrast, the acn/water curve experiences a sharp drop until $x_{\text{H}_2\text{O}} \approx 0.1$ after which it gradually increases to the value in pure water. The initial drop can be attributed to the formation of H bonds accepted by H_2O , as will be shown next.

The qualitative difference between the ANF and dM-ANF curves for low water content is borne out by the amino ^1H NMR chemical shift as function of composition, Figure 9. It is well-known that a proton resonance moves downfield when the corresponding nucleus enters into a hydrogen bond⁴⁵ even though the different contributions to this effect are rarely understood quantitatively. Thus, $\delta H_{(\text{N})} = 5.12 \text{ ppm}$ for ANF in pure acn, which forms only weak H bonds, and it moves to

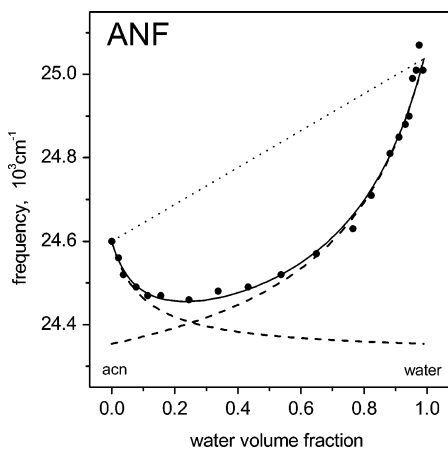


Figure 10. Absorption frequency of the ANF absorption band in acetonitrile/water (full circles) from Figure 7a. The fit (solid line) involves $\text{H}_2\text{O}\cdots\text{H}-\text{N}$ hydrogen bonding and stepwise $\text{CH}_3\text{CN} \rightarrow \text{H}_2\text{O}$ exchange around the solute. Dashed lines show the spectral shifts by these contributions separately.

$\delta H_{(\text{N})} = 5.92$ ppm in pure dmsO, which is a strong H-bond acceptor. The same direction is noted when a small amount of water is added to an ANF/acn solution, from 5.12 to an extremum of 5.20 ppm at water volume fraction of about 0.1. For higher water content, the chemical shift of the amino proton moves parallel to $\delta H_{(\text{C}_5)}$ of an aromatic reference proton, due changes in the bulk dielectric properties.⁴⁶ The observation is consistent with an initial formation of an H bond accepted by an H_2O solvent molecule. On the other hand, in dmsO a different direction is observed when water is added: upfield with a slope which exceeds that for the aromatic reference proton. This observation suggests that a strong $\text{Me}_2\text{SO}\cdots\text{HN}-$ bond is replaced by a weaker $\text{H}_2\text{O}\cdots\text{HN}-$ bond.

Let us return to the absorption band of ANF in acn/water, shown in the upper part of Figure 7a, which is reproduced on an expanded vertical scale in Figure 10. The band position in pure acn is lowered sharply upon addition of small amounts of water. The initial lowering was assigned by ^1H NMR spectroscopy (Figure 9) to amino H bonds being accepted by H_2O molecules. After the H-bonding sites are saturated, a curved blue shift of the absorption spectrum is observed until the pure water solution is reached. The positive curvature is indicative of preferential solvation by acn in the mixture. The effects of hydrogen bonding and preferential absorption can be described by sigmoidal binding terms⁴⁷

$$\tilde{\nu}_x = \tilde{\nu}_{\text{acn}} + m \tilde{\chi}_{\text{HB}} \frac{k_{\text{HB}} y}{1 + k_{\text{HB}} y} + n \tilde{\chi}_{\text{SSE}} \frac{k_{\text{SSE}} y}{1 + k_{\text{SSE}} y} \quad (11)$$

with $y = x_{\text{H}_2\text{O}}/(1 - x_{\text{H}_2\text{O}})$. The last term describes stepwise solvent exchange (SSE)¹⁶ of n acetonitrile volume partitions around the solute by water, each accompanied by a positive frequency shift, $\tilde{\chi}$; the exchange constant for a single site is k . The second term describes m hydrogen-bonding sites in the same manner. The total shift $\tilde{\nu}_{\text{acn}} - \tilde{\nu}_{\text{water}} = m \tilde{\chi}_{\text{HB}} + n \tilde{\chi}_{\text{SSE}}$ is measured directly so that of the four effective parameters, $m \tilde{\chi}_{\text{HB}}$, $n \tilde{\chi}_{\text{SSE}}$, k_{HB} , and k_{SSE} , only three remain. The search may be limited further because the free enthalpy of transfer from acn to water, $\Delta_{\text{acn}\rightarrow\text{water}}G = -RT(m \ln k_{\text{HB}} + n \ln k_{\text{SSE}})$, can be estimated from solubilities. With $m = 2$ from structural considerations, we obtain $n = 14$, $\tilde{\chi}_{\text{HB}} = -123 \text{ cm}^{-1}$, $\tilde{\chi}_{\text{SSE}} = +51 \text{ cm}^{-1}$, $\ln k_{\text{HB}} = +2.42$, $\ln k_{\text{SSE}} = -1.488$. The resultant curve is shown as a solid line in Figure 10, and limiting behavior is shown as dashed lines. The constant k_{HB} for hydrogen-bond

exchange $\text{MeCN}\cdots\text{H}_2\text{N}- + \text{H}_2\text{O} \rightarrow \text{H}_2\text{O}\cdots\text{H}_2\text{N}- + \text{MeCN}$ at a single site corresponds to $\Delta_{\text{HB}}G = -RT 2.42 = -6 \text{ kJ/mol}$. This value may be compared with quantum-chemical calculations for the strength of a hydrogen bond in the gas phase,⁴⁸ which give $\Delta_{\text{HB}}G = -4.9 \text{ kJ/mol}$ for the exchange at aniline.⁴⁹ The amino hydrogen atoms in ANF are more polarized, which explains the stronger hydrogen bond in this case. The number $n + m$ of sites around the solute is consistent with the volume of the first solvent shell and the molar volumes of acn and water. The application of this model to all examined solvent mixtures is currently being studied.

4. Conclusions

Optical spectra of polarity probes, which are strongly solvatochromic, should be described by optical band shapes for absorption and emission, rather than by the peak position of the absorption spectrum or fluorescence quantum distribution. Band positions are best determined by quantitative comparison with the band shape in an aliphatic reference solvent. The difference between the two approaches was demonstrated with an aliphatically substituted 2-amino-7-nitro-fluorene. Small spectral changes of the parent compound in aqueous mixtures can be divided into binding curves for hydrogen bonding and for stepwise solvent exchange. Band-shape parameters are provided for amino-nitro-fluorenes that will be used as probes for coherent solvent dynamics on a femtosecond time scale.

Acknowledgment. We thank the Deutsche Forschungsgemeinschaft and the Fonds der chemischen Industrie for support, C. Mügge and S. A. Kovalenko for measurements, B. Kirchner for quantum-chemical calculations, U. Resch-Genger and the Bundesanstalt für Materialforschung (BAM) for standard fluorescence spectra, and M. Maroncelli for fruitful discussions. G.S. is grateful to the Humboldt Foundation for a scholarship.

Supporting Information Available: Procedure for decomposition of fs transient absorption spectra, spectral contributions for dM-ANF in acetonitrile at late time, lognormal descriptions of all stationary optical spectra, solvatochromic plot of dM-ANF, and X-ray crystal structure of ANF. This material is available free of charge via the Internet at <http://pubs.acs.org>.

References and Notes

- (1) Lippert, E. Z. *Elektrochem.* **1957**, *61*, 962.
- (2) Baumann, W.; Bischof, H. *J. Mol. Struct.* **1985**, *129*, 125.
- (3) Czekalla, J.; Liptay, W.; Meyer, K. O. Z. *Elektrochem.* **1963**, *67*, 465.
- (4) Fu, W.; Feng, J. -K.; Pan, G. -B. *J. Mol. Struct.: THEOCHEM* **2001**, *545*, 157.
- (5) (a) Catalán, J.; López, V.; Pérez, P.; Villamil, R. M.; Rodríguez, J.-G. *Liebigs Ann.* **1995**, 241. (b) Catalán, J.; López, V.; Pérez, P. *Liebigs Ann.* **1995**, 793.
- (6) Hallidy, L. A.; Topp, M. R. *J. Phys. Chem.* **1978**, *82*, 2415.
- (7) Mandal, P. K.; Sarkar, M.; Samanta, A. *J. Phys. Chem. A* **2004**, *108*, 9048.
- (8) Hu, Z.; Margulis, C. J. *J. Phys. Chem. B* **2006**, *110*, 11025.
- (9) Ruthmann, J.; Kovalenko, S. A.; Ernsting, N. P.; Ouw, D. *J. Chem. Phys.* **1998**, *109*, 5466.
- (10) Mühlpfordt, A.; Schanz, R.; Ernsting, N. P.; Farztdinov, V.; Grimme, S. *Phys. Chem. Chem. Phys.* **1999**, *1*, 3209.
- (11) Lustres, J. L. P.; Kovalenko, S. A.; Mosquera, M.; Senyushkina, T.; Flasche, W.; Ernsting, N. P. *Angew. Chem., Int. Ed.* **2005**, *44*, 5635.
- (12) Dobryakov, A. L.; Kovalenko, S. A.; Ernsting, N. P. *J. Chem. Phys.* **2003**, *119*, 988.
- (13) Dobryakov, A. L.; Kovalenko, S. A.; Ernsting, N. P. *J. Chem. Phys.* **2005**, *123*, 044502.
- (14) Hsu, C.-P.; Song, X.; Marcus, R. A. *J. Phys. Chem. B* **1997**, *101*, 2546.
- (15) Fee, R. S.; Maroncelli, M. *Chem. Phys.* **1994**, *183*, 235.

- (16) (a) Covington, A. K.; Lilley, T. H.; Newman, K. E.; Porthouse, G. *A. J. Chem. Soc., Faraday Trans. 1* **1973**, *69*, 963. (b) Covington, A. K.; Dunn, M. *J. Chem. Soc., Faraday Trans. 1* **1989**, *85*, 2827.
- (17) Saroja, G.; Pingzhu, Z.; Ernsting, N. P.; Liebscher, J. *J. Org. Chem.* **2004**, *69*, 987.
- (18) Marcus, Y. *Solvent Mixtures: Properties and Selective Solvation*; Marcel Dekker Inc.: New York, 2002; Tables 2.16 and 2.17F.
- (19) Gardecki, J. A.; Maroncelli, M. *Appl. Spectrosc.* **1998**, *52*, 1179.
- (20) Birks, J. B. *Photophysics of Aromatic Molecules*; Wiley-Interscience: New York, 1970.
- (21) Siano, D. B.; Metzler, D. E. *J. Chem. Phys.* **1969**, *51*, 1856.
- (22) The emission lineshape of dBdP-ANF was used throughout. A more-detailed treatment applies for excitation at the red edge of the absorption band¹⁵.
- (23) Mataga, N.; Kubota, T. In *Molecular Interactions & Electronic Spectra*; MerceL Dekker: New York, 1970; p 371.
- (24) Song, X.; Chandler, D. *J. Chem. Phys.* **1998**, *108*, 2594.
- (25) (a) Cortés, J.; Heitele, H.; Jortner, J. *J. Phys. Chem.* **1994**, *98*, 2527. (b) Horng, M. L.; Gardecki, J. A.; Papazyan, A.; Maroncelli, M. *J. Phys. Chem.* **1995**, *99*, 17311.
- (26) (a) Ooshika, Y. *J. Phys. Soc. Jpn.* **1954**, *9*, 594. (b) Lippert, E. *Z. Naturforsch.* **1955**, *A10*, 541. (c) McRae, E. G. *J. Phys. Chem.* **1957**, *61*, 562.
- (27) Amos, A. T.; Burrows, B. L. *Adv. Quantum Chem.* **1973**, *7*, 289.
- (28) (a) Tassaing, T.; Danten, Y.; Besnard, M.; Zoidis, E.; Yarwood, J. *Chem. Phys.* **1994**, *184*, 225. (b) Venables, D. S.; Schmuttenmaer, C. A. *J. Chem. Phys.* **1998**, *108*, 4935.
- (29) Marcus, Y.; Kamlet, M. J.; Taft, R. W. *J. Phys. Chem.* **1988**, *92*, 3613.
- (30) Kamlet, M. J.; Abboud, J. L. M.; Abraham, M. H.; Taft, R. W. *J. Org. Chem.* **1983**, *48*, 2877.
- (31) When plotted against mole fraction x' , the resultant curve is bent. Excellent linearity (to within measurement error) with volume fraction x proves that the latter is the appropriate compositional measure.
- (32) Maroncelli, M.; Fleming, G. R. *J. Chem. Phys.* **1987**, *86*, 6221.
- (33) (a) Marcus, Y. *Aust. J. Chem.*, **1983**, *36*, 1719. (b) Marcus, Y. *J. Chem. Soc., Faraday Trans. 1* **1988**, *84*, 1465.
- (34) Nagy, O. B.; Muanda, M. w. Nagy, J. B. *J. Phys. Chem.* **1979**, *83*, 1961.
- (35) (a) Kirkwood, J. G.; Buff, P. F. *J. Chem. Phys.* **1951**, *19*, 774. (b) Ben-Naim, A. *Cell Biophys.* **1988**, *12*, 255. (c) Ben-Naim, A. *J. Phys. Chem.* **1989**, *93*, 3809.
- (36) Suppan, P. *J. Chem. Soc., Faraday Trans. 1* **1987**, *83*, 495.
- (37) Provided that specific effects are absent. The statement also holds in the present case because, for dM-ANF, no specific solvation mode exists that could cause a red-shift of the absorption band.
- (38) A background due to Mie scattering of remaining particles could not be fully controlled in these experiments. This is why the absorption center frequency in this region is determined only approximately and quantitative analysis must be deferred.
- (39) Jacques, P. *J. Phys. Chem.* **1986**, *90*, 5535.
- (40) Harrison, W. J.; Mateer, D. L.; Tiddy, G. J. T. *J. Phys. Chem.* **1996**, *100*, 2310.
- (41) Bertie, J. E.; Lan, Z. *J. Phys. Chem. B* **1997**, *101*, 4111.
- (42) Bergman, D. L.; Laaksonen, A. *Phys. Rev. E* **1998**, *58*, 4706.
- (43) Goldammer, E.v.; Hertz, H. G. *J. Phys. Chem.* **1970**, *74*, 3734.
- (44) Özal, T. A.; van der Vegt, N. F. A. *J. Phys. Chem B* **2006**, *110*, 12104.
- (45) Tucker, E. E.; Lippert, E. In *The Hydrogen Bond*; Schuster, P., Zundel, G., Sandorfy, C., Eds.; North Holland Publ. Comp.: Amsterdam, 1976; Chapter 17.
- (46) Golubev, N. S.; Denisov, G. S.; Smirnov, S. N.; Shchepkin, D. N.; Limbach, H.-H. *Z. Phys. Chem.* **1996**, *196*, 73.
- (47) Klotz, I. M. *Ligand-Receptor Energetics*; John Wiley & Sons, Inc.: New York, 1997; p 22.
- (48) Thar, J.; Kirchner, B. *J. Phys. Chem. A* **2006**, *110*, 4229.
- (49) Kirchner, B., to be submitted for publication.